Multi-stage Distance Prediction For Rear End Collision Risk Assessment

Anthony Chassignet, Thomas Sproesser, and Michel Basset*

Abstract— **One of the challenges in developing autonomous vehicles is the coexistence of both type of vehicles, autonomous and human-driven vehicles. In this paper, we consider the rear-end collision risk between a human-driven vehicle (Ego) and an autonomous vehicle (Front). Unlike autonomous vehicles, whose braking is determined by an algorithm, the braking of a human-driven vehicle depends on the individual reaction of the driver and is not known in advance. This article presents a new model of human-driver deceleration prediction. The model depends on the danger perception of the driver, which is measured by a new indicator I_{Hazard}. Because rear-end collision risk depends on the distances travelled by Front and Ego since the start of braking, a new travelled distance prediction method is presented.**

I. INTRODUCTION

The large-scale deployment of autonomous vehicles is expected in the near future; however, a prolonged transition phase is anticipated, during which time autonomous and human-driven vehicles will coexist in the same traffic environment. Advanced Driver Assistance Systems (ADAS) are regarded as a key technology for modern vehicle control and safety and are essential for the development of autonomous driving [1].

Such cohabitation may lead to conflict-prone situations and heightened safety challenges, since the behaviour of autonomous vehicles is deterministic, being governed by algorithms, whereas human driving behaviour is inherently stochastic. Human responses depend on various factors, such as the current traffic situation, environmental conditions (e.g., weather, time of day), physiological states (e.g., fatigue, attention), driving experience, age, gender, and cultural background (see, for instance, [2]–[3]).

To support the development of new ADAS, there is a need for a real-time road risk assessment tool. In this paper, risk is defined as the probability of an unwanted event occurring. Assuming that road risk can be decomposed into elementary risks (e.g., loss of control, rear-end collision), this study focuses on assessing the risk of a rear-end collision between a leading vehicle, hereafter referred to as Front, and a following vehicle, referred to as Ego, under the assumption that the Front vehicle initiates a braking manoeuvre.

In this study, we assume that at least one of the two vehicles is driven by a human driver. The objective is therefore to predict the braking behaviour of the human driver(s). Two scenarios are considered. Case 1: the Ego vehicle is autonomous, while the Front vehicle is driven by a human. The objective is to provide the Ego vehicle with an estimate of the braking action expected from the Front vehicle. This information could be transmitted via a Vehicular Ad Hoc Network (VANET)-based inter-vehicle communication system. Case 2: the Ego vehicle is driven by a human driver. In this case, the Ego vehicle's ADAS must intervene when the risk of collision exceeds a critical threshold.

In both cases, whether it is an autonomous vehicle (case 1) or an ADAS (case 2), Ego must know what the human-driven vehicle is going to do. For simplicity, the remainder of this paper considers the Ego vehicle as human-driven and the Front vehicle as autonomous.

When assessing rear-end collision risk, defined as the probability of two vehicles colliding, the main challenge lies in estimating how the future evolution of the deceleration profiles of both vehicles will evolve over a short time. In addition, the reaction time of the Ego driver must also be estimated. This reaction time can be inferred using a Bayesian network; the reader is referred to the work of Russo [4] for further details. Once the braking estimates are available, the travelled distances of both vehicles can be predicted, and consequently, the probability of a collision occurring within the considered prediction horizon can be evaluated.

This paper presents a novel braking prediction method (Section V), based on a new hazard indicator I_{Hazard} introduced in Section III and on a dedicated experimental test campaign used for statistical analysis (Section IV). Building on this indicator and the proposed braking model, a new multi-stage method for estimating travelled distances is developed in Section VI. This method provides a prediction horizon of up to 1.5 seconds. Finally, experimental results obtained using our instrumented vehicles are presented in Section VII, followed by conclusions and perspectives in Section VIII.

II. RELATED WORK

Travelled distance is commonly used as a measure of exposure in road risk estimation for Advanced Driver Assistance Systems (ADAS). Predicting this quantity over a finite horizon enables anticipation of potentially hazardous situations and allows assistance and warning strategies to be adapted proactively [5].

A significant part of ADAS research relies on predicting vehicle trajectories or speed profiles, from which future travelled distance is obtained by integration. Model-based approaches typically employ longitudinal or kinematic vehicle models and are often embedded within predictive planning or control frameworks [6]. These methods are interpretable and compatible with safety constraints; however, their

*All authors are with the IRIMAS Laboratory, University of Haute Alsace, Mulhouse, France (corresponding author to provide phone: +33 3 89 33 69 31; e-mail: name.surname@uha.fr)

performance strongly depends on accurate knowledge of the future driving context and driver behaviour.

To capture the uncertainty inherent in driving, probabilistic approaches have been introduced for motion prediction and risk assessment. Bayesian filters, Markov models, and probabilistic occupancy grid-based methods are commonly used to estimate the distributions of future trajectories and velocities in complex traffic environments [7]-[9]. These approaches naturally allow the integration of risk indicators such as Time To Collision (TTC) or the probability of dangerous interactions.

More recently, deep learning methods have been developed within the ADAS domain, particularly for predicting multi-modal trajectories and estimating risk based on data from on-board sensors [10]-[12]. While these approaches often achieve high predictive performance, they rely on models that are difficult to interpret and do not always ensure the physical consistency of the predicted quantities, which limits their applicability in safety-critical systems.

III. Hazard indicator

The method presented in this work assumes that there is a correlation between the perceived level of danger and the intensity of the braking response when the Ego vehicle begins to brake. Accordingly, an indicator representing the level of danger is required.

Time To Collision (TTC) and Modified Time To Collision (MTTC) are well-established indicators. These metrics assume that the speeds (TTC) or accelerations (MTTC) of both the Front and Ego vehicles remain constant until a potential collision occurs. When the predicted time to collision is very short and the driver has limited opportunity to react, these indicators provide a reliable measure of danger. However, for longer prediction horizons, the driver has more time to adjust vehicle speed, weakening the correlation between the indicators and the actual risk. Indeed, beyond a certain threshold, the Ego vehicle may avoid the collision entirely. Another limitation arises when both vehicles travel at constant speeds. In such cases, these indicators may fail to signal an impending collision, even though a real danger exists if the inter-vehicle distance is less than the reaction distance required to avoid a collision in the event of braking by the Front vehicle.

The indicator proposed here, see (1), uses instantaneous measurements of speed and acceleration, as well as the distance between Front and Ego (D_{inter}) at the moment of analysis $t = t_i$:

$$I_{\text{Hazard}} = \frac{v_{\text{Ego}} \times 1s + (v_{\text{Ego}} - v_{\text{Front}}) \times p_1 + (a_{\text{Ego}} - a_{\text{Front}}) \times p_2}{D_{\text{inter}}} \quad (1)$$

The proposed hazard indicator I_{Hazard} is defined as the ratio between vehicle speed (multiplied by one second to obtain a dimensionless quantity) and the inter-vehicle distance. For a given distance, higher speeds correspond to higher perceived danger. This value is weighted by the differences in speed and acceleration between the two vehicles: the greater the braking intensity of the Front vehicle relative to the Ego vehicle, the higher the associated danger.

These two differences are weighted by the two factors p_1 and p_2, which account for the driver's perception of danger. Indeed, it is the perceived rather than the objective danger that drives human behaviour. Our analysis indicates that the indicator is sensitive to differences in acceleration; however, for large inter-vehicle distances, the perception of acceleration differences is low. Consequently, the p_2 factor should be modelled as a decreasing function of distance. In the present study, this sensitivity has not yet been optimised and will be addressed in future work. For the time being, p_1 and p_2 are treated as constant parameters (p_1 = 1s and p_2 = 1s²).

To validate that the indicator accurately reflects danger, the collision rate was calculated for varying values of D_{inter}, v_{Ego} and v_{Front}. Both vehicles were assumed to initiate emergency braking (a = -9m/s²) and the value of I_{Hazard} was evaluated using the dynamic values immediately before braking starts. The result (see Fig. 1) demonstrates a strictly monotonic relationship between I_{Hazard} and the danger (expressed by the collision rate), a necessary condition for using this indicator to assess the rear-end collision risk. Further details on the numerical interpretation of this indicator are provided in Section V.

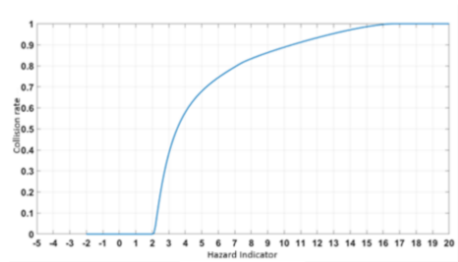

Figure 1. Collision rates according to the value of the danger indicator

IV. Data generation for modelling

The model presented in this paper is based on experimental data in which drivers reactions were measured during real tests. These reactions primarily concern reaction time and braking strategy, i.e. how drivers decelerate during the braking phase.

The experimental data were obtained using two complementary approaches. The first approach employs a driving simulator, consisting of a car seat, steering wheel, dashboard, and all necessary driving controls, including accelerator, brake, and clutch pedals. Three screens positioned in front of the dashboard provide an immersive view of the scrolling road environment. The simulator records driver inputs, such as steering wheel angle and brake pedal pressure, and integrates them in real time into the simulated road scenario. As our laboratory does not have such a driving simulator, a collaboration with the LAMIH research laboratory in Valenciennes have been initiated in order to access their simulator.

The second approach involves on-road testing, in which drivers operate instrumented vehicles alongside other road users on public roads. Two test vehicles from our laboratory were used for these experiments. The first, a Renault Scenic, is fully equipped with an inertial measurement unit (IMU), GPS, camera, and LiDAR sensors. The second, a Skoda, is equipped with an IMU and GPS antenna. Sensor data were collected and recorded using RTMaps software. To synchronize measurement files from both vehicles, a common time reference is defined using Coordinated Universal Time (UTC).

Both approaches have distinct advantages and limitations. Compared to open-road testing, the driving simulator allows driver reactions to be evaluated in traffic situations involving potential hazards. Moreover, test scenarios can be reproduced in a controlled and repeatable manner. A simulated scenario consists of a sequence of intersections and braking manoeuvres performed by the Front vehicle and displayed on the screens. These braking manoeuvres vary in both intensity and temporal profile and are uploaded to the simulator before the start of the experimental campaign. Importantly, these data are not generated by simulation; rather, the speed and deceleration profiles are collected beforehand from real-world driving experiments using one of our instrumented vehicles. However, the braking actions performed by the Ego driver in the simulator exhibit certain biases. These biases are particularly noticeable during the final phase of braking, when the vehicle is coming to a stop in scenarios that do not involve any immediate danger. In contrast, open-road experiments provide more realistic and accurate driver behaviour for this type of low-risk braking. Then, the necessary tests for braking characterised by $I_{\text{Hazard}} \leq 1.5$ are carried out on open roads, while the data for $I_{\text{Hazard}} > 1.5$ are obtained using the simulator.

V. DECELERATION MODEL

The model proposed in this paper is probabilistic in nature and is based on the hypothesis that a driver decelerates in a similar manner when faced with comparable driving situations. The similarity between situations is characterized using the hazard indicator I_{Hazard}. The objective of the model is to capture the correlation between the driver's response - i.e. the deceleration $a(t)$ - and the time evolution of $I_{\text{Hazard}}(t)$.

Since braking represents the driver's response to the perceived level of the danger of a situation, instantaneous values of $a(t_i)$ and $I_{\text{Hazard}}(t_i)$ are not considered. Instead, the deceleration is analysed over a sliding time window (the duration of which is discussed below). For consistency, the value of I_{Hazard} associated with a given braking response (hence the deceleration) is evaluated at the beginning of this interval, after compensating for the driver's reaction time. This approach allows the model to map the driver's subjective perception of danger to the numerical value of the indicator. To account for differences in driving behaviour, individual probability laws have been identified for two different drivers.

For modelling purposes, the I_{Hazard} function is quantified, i.e. its range of possible values is divided into intervals, called classes. Within each time window, the deceleration profile is approximated by a straight line obtained by minimizing a least-squares criterion. The slope of this line thus corresponds to the average jerk over the interval in the least-squares sense.

In a subsequent step, the resulting linear approximations are grouped according to their corresponding I_{Hazard} classes. For each class of I_{Hazard}, two histograms are constructed using the average jerk over the interval values along the x-axis: one gathering decelerations when the last measured jerk $J(t_i)$ is positive, one when it is strictly negative. These histograms are then approximated by normal distributions $\mathcal{N}(\mu, \sigma^2)$ using maximum likelihood estimation. One example of jerk histogram is presented in Fig. 2, and the identified probability laws are presented in Table I and Table II.

The choice of time-window length involves a trade-off. On the one hand, the interval must be short enough to ensure modelling accuracy, on the other hand, it must be long enough to give an ADAS with adequate time to avoid a potential collision or, at least, to mitigate its consequences. The proposed strategy is therefore to prioritise accuracy by selecting a short interval (ΔT = 500ms) and embedding the resulting model within a sequential multi-stage framework that extends the prediction horizon by integer multiples of ΔT. In the experimental results (Section VII), the prediction horizon covers 1.5s, which is generally sufficient for urban driving and remains beneficial in other driving contexts.

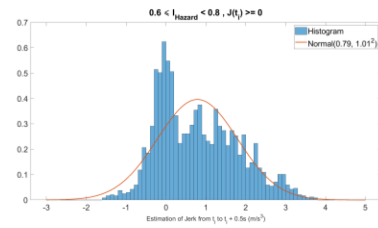

Figure 2: Histogram of jerk for $0.6 \leq I_{\text{Hazard}} < 0.8$ and $J(t_i) \geq 0$

TABLE I. DRIVER 1 PROBABILITY LAWS

Hazard class	$J(t_i) < 0$		$J(t_i) \geq 0$	
	μ	σ	μ	σ
$-1 < I_{\text{Hazard}} < 0$	-0.02	0.46	0.33	0.32
$0 < I_{\text{Hazard}} < 0.4$	0.16	0.72	0.86	1.13
$0.4 < I_{\text{Hazard}} < 0.6$	0.08	0.70	1.16	1.17
$0.6 < I_{\text{Hazard}} < 0.8$	-0.23	0.76	0.79	1.01
$0.8 < I_{\text{Hazard}} < 1$	-0.31	0.89	0.26	0.82

TABLE II. DRIVER 2 PROBABILITY LAWS

Hazard class	$J(t_i) < 0$		$J(t_i) \geq 0$	
	μ	σ	μ	σ
$-1 < I_{\text{Hazard}} < 0$	1.96	0.15	3.04	1.68
$0 < I_{\text{Hazard}} < 0.4$	0.12	0.67	1.25	1.34
$0.4 < I_{\text{Hazard}} < 0.6$	-0.4	0.74	0.23	0.98
$0.6 < I_{\text{Hazard}} < 0.8$	-0.58	0.77	0.3	0.63
$0.8 < I_{\text{Hazard}} < 1$	-0.8	0.69	-0.05	0.33

VI. NEW BRAKING AND TRAVELLED DISTANCE PREDICTION

The model presented in the previous section can be used as the core component of a procedure that provides an estimate of the distance travelled over the next time interval and, furthermore, enables an extension of the prediction horizon for both deceleration and travelled distance.

For the purpose of rear-end collision risk assessment, it is essential to estimate the distances that both vehicles are expected to travel in the near future. The difference between these two predicted distances, combined with the initial inter-vehicle distance (i.e., the current distance $D_{\text{inter}}(t_i)$), can then be used to compute the probability of a collision. More specifically, during the operational phase, the algorithm evaluates, at each analysis instant $t = t_i$, the value of the hazard indicator $I_{\text{Hazard}}(t_i)$ and the sign of the jerk, given by sign($a(t_i) - a(t_{i-1})$). The braking prediction model then provides the probability density function of the jerk J.

Using this probability density function, together with the last available measurement of the Ego vehicle deceleration $a_{\text{Ego}}(t_i)$, it becomes possible to estimate the probability distribution of the predicted deceleration $a_{\text{Ego,pred}}$ over the next time interval (ΔT = 500ms), as well as the corresponding travelled distance over the same interval (see (2)).

$$a_{\text{Ego,pred}}(t_{i+1}) = J.\Delta T + a_{\text{Ego}}(t_i) \tag{2}$$

The estimated braking profiles and travelled distances can now be incorporated into a multi-stage procedure to increase the prediction horizon. Given the predicted values of $v_{\text{Ego}}(t_{i+1})$ and the travelled distance by Ego $d_{\text{Ego}}(t_{i+1})$, together with the corresponding predictions for the Front vehicle (see note below), the inter-vehicle distance $D_{\text{inter}}(t_{i+1})$ can be estimated and, consequently, the hazard indicator $I_{\text{Hazard}}(t_{i+1})$ can be updated. This updated information is then used to predict the subsequent braking action $a_{Ego}(t_{i+2})$. By iterating this process, the prediction horizon can be extended over multiple integers of ΔT. Naturally, prediction uncertainty increases with the length of the prediction horizon.

Regarding the Front vehicle data, two situations may be considered. Either the Front vehicle's speed $v_{Front}(t_i)$ and deceleration $a_{\text{Front}}(t_i)$ must be estimated using the Ego vehicle's sensors (e.g., LiDAR), in which case assumptions about the Front driver's braking strategy are required; or the Front vehicle transmits this information directly, in particular its braking model (i.e. jerk probability laws), when a Vehicular Ad Hoc Network (VANET) is available. The latter case leads to a substantial improvement in prediction accuracy.

VII. Experiments and Results

To evaluate the proposed braking estimator, on-road experiments were conducted in the Mulhouse metropolitan area. This experimental campaign involved urban driving scenarios in which the two test vehicles followed one another in real traffic conditions.

The first illustrative example corresponds to a situation in which the Front vehicle (Skoda) enters a roundabout, followed by the Ego vehicle (Renault). Fig. 3 and 4 depict the corresponding temporal evolution of vehicles speed and acceleration (Fig. 3), as well as the inter-vehicle distance D_{inter} and the hazard indicator I_{Hazard} (Fig. 4). In this experiment, $I_{\text{Hazard,Front}}$ is transmitted to the Ego vehicle by the Front vehicle via a VANET communication link. The time axis is referenced to the instant at which braking by the Ego vehicle is detected, defined as the moment when the deceleration exceeds a threshold of 1m/s².

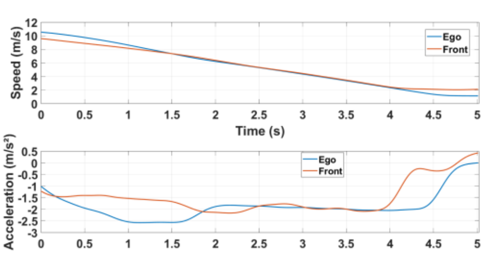

Figure 3: Temporal evolution of measures of speed and acceleration

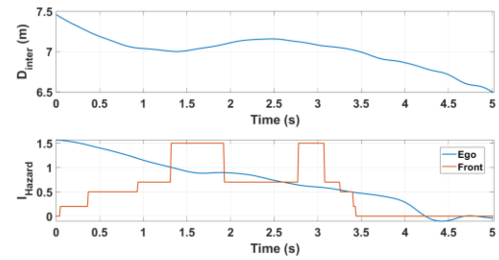

Figure 4: Temporal evolution of D_{inter} and I_{Hazard}

Since this is an offline analysis, we can compare the predictions, i.e. how the driver is likely to brake over the next 1.5s with the braking actions that the driver actually performed. For this comparison, the prediction horizon is divided into three intervals of 0.5s each (Fig. 5 for the 1st interval, Fig. 7 for the 2nd interval and Fig. 9 for the 3rd interval), and we compare the deceleration at the end of each interval. Then, by double integration, we can compare the travelled distance prediction with the real travelled distance during the interval (Fig. 6 for the 1st interval and Fig. 8 for the 2nd interval and Fig. 10 for the 3rd interval).

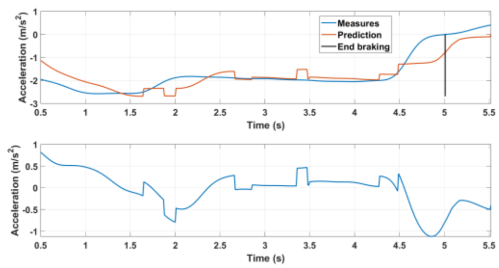

Figure 5: (a) Comparison of the deceleration prediction for the 1st interval (b) Absolute error of prediction

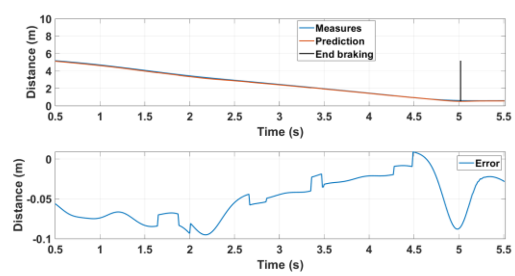

Figure 6: (a) Comparison of the travelled distance prediction for the 1st interval (b) Absolute error of prediction

Until $t = 4.5$s, the absolute deceleration error remains within ± 1m/s² (Fig. 6). Beyond this point, the error increases as the driver prepares for re-acceleration. In fact, the braking prediction model was developed to predict braking until the vehicle stops. However, the model cannot predict situations in which driver accelerates again without firs stopping.

For the first prediction interval, the travelled distance prediction error is inferior to 0.1m. These results indicate that the proposed model is capable of accurately predicting short-term braking behaviour and its kinematic consequences, which is a key requirement for real-time rear-end collision risk assessment.

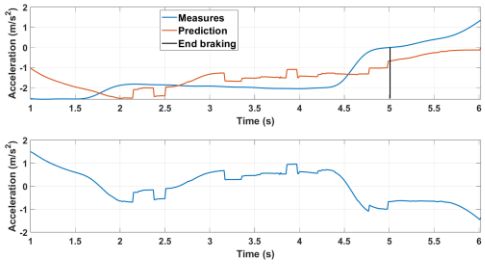

Figure 7: (a) Comparison of the deceleration prediction for the 2nd interval (b) Absolute error of prediction

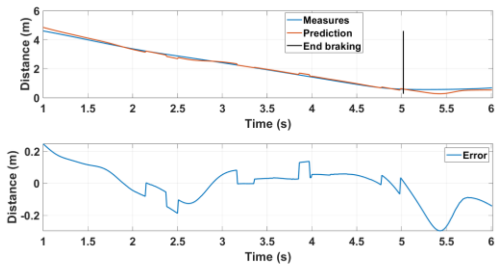

Figure 8: (a) Comparison of the travelled distance prediction for the 2nd interval (b) Absolute error of prediction

For the 2nd time interval (Fig. 7), excepted at the beginning, the absolute deceleration error remains within ± 1m/s² until $t = 5$s. Beyond this point, the error increases as the driver prepares for re-acceleration. The travelled distance prediction error remains within ± 0.2m (Fig. 8). From the 2nd interval onwards, uncertainties increase due to the accumulation of uncertainties.

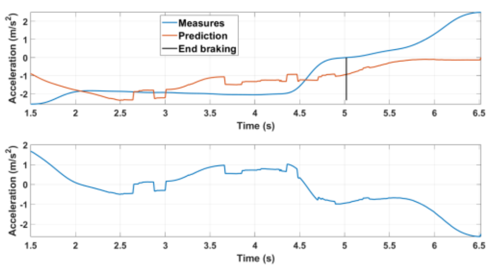

Figure 9: (a) Comparison of the deceleration prediction for the 3rd interval (b) Absolute error of prediction

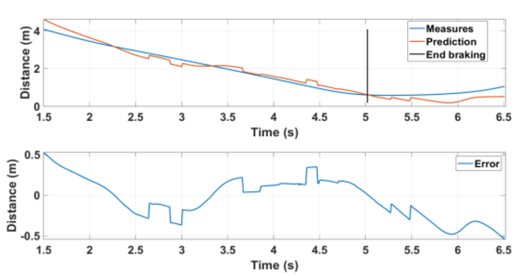

Figure 10: (a) Comparison of the travelled distance prediction for the 3rd interval (b) Absolute error of prediction

For the 3rd interval, the absolute deceleration error remains within ± 2m/s² (Fig. 9). Although the deceleration error seems to be slightly high, the impact on the travelled distance prediction error remains within ± 0.5m (Fig. 10). The impact of the error of deceleration prediction is limited because the time interval duration is only of 500ms.

As a second example, we consider the following sequence where Front (Renault), followed by Ego (Skoda), is approaching a pedestrian crossing path. As previously, Fig. 11 and Fig. 12 show the evolution of velocity and acceleration, as well as those of D_{inter} and I_{Hazard}.

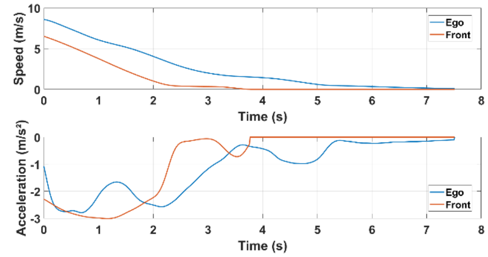

Figure 11 : Temporal evolution of D_{inter} and I_{Hazard}

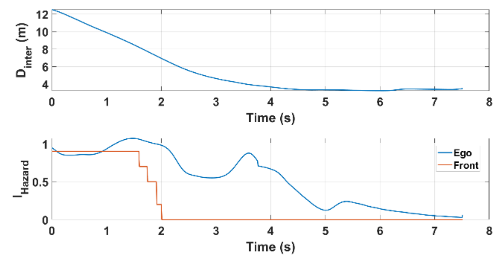

Figure 12: Temporal evolution of D_{inter} and I_{Hazard}

For the 1st interval, excepted for the beginning, the deceleration prediction error remains within ±1m/s² (Fig. 13), and the travelled distance prediction error remains within ±0.1m (Fig. 14).

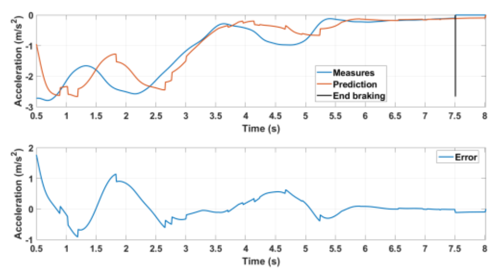

Figure 13: (a) Comparison of the deceleration prediction for the 1st interval (b) Absolute error of prediction

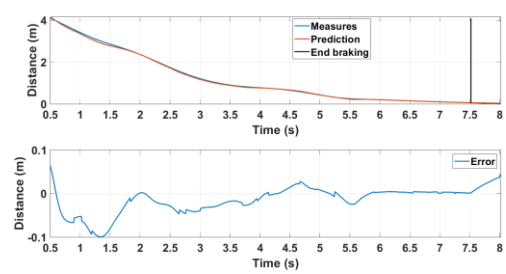

Figure 14: (a) Comparison of the travelled distance prediction for the 1st interval (b) Absolute error of prediction

For the 2nd interval, excepted for the first 0.1s ($t = 0.5$s to $t = 0.6$s), the deceleration prediction error remains within ±1m/s² (Fig. 15), and the travelled distance prediction error remains within ±0.2m (Fig. 16).

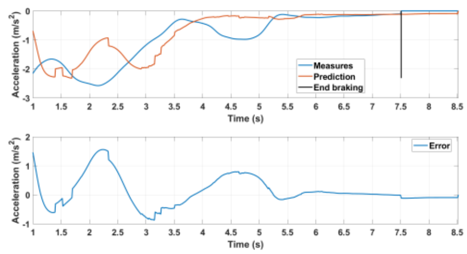

Figure 15: (a) Comparison of the deceleration prediction for the 2nd interval (b) Absolute error of prediction

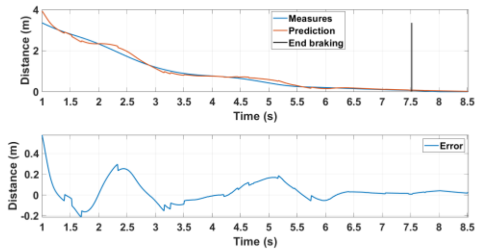

Figure 16: (a) Comparison of the travelled distance prediction for the 2nd interval (b) Absolute error of prediction

For the 3rd interval, the error of deceleration prediction mainly remains within ± 1m/s² (Fig. 17), while the travelled distance is evolving between -0.2m and 0.5m (Fig. 18).

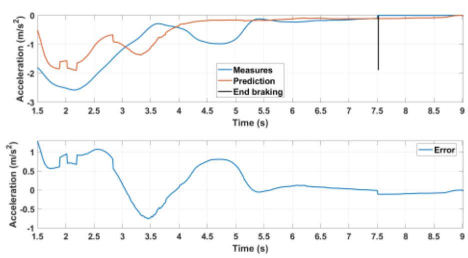

Figure 17: (a) Comparison of the deceleration prediction for the 3rd interval (b) Absolute error of prediction

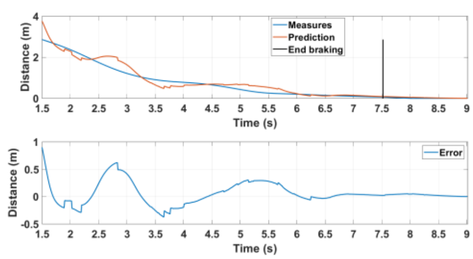

Figure 18: (a) Comparison of the travelled distance prediction for the 3rd interval (b) Absolute error of prediction

As similar results were obtained for both drivers, only the mean errors for Driver 1 are presented. Considering all its braking events, the mean prediction error for the 1st interval is 0.27m/s² (root mean square error (RMSE) = 0.62m/s²) for deceleration and - 0.02m (RMSE = 0.04m) for the travelled distance. For the 2nd interval the errors are 0.43m/s² (RMSE = 1m/s²) and 0.08m (RMSE = 0.16m). Finally, for the 3rd interval the errors are 0.44m/s² (RMSE = 1.16m/s²) and 0.16m (RMSE = 0.38m). This result shows that the prediction error increases with the number of intervals, it reflects the progressive accumulation of model uncertainty.

VIII. Conclusion

This paper presents a novel method for estimating the forthcoming travelled distance of an Ego vehicle following a braking Front vehicle has been presented. This method relies on a new deceleration prediction model with a prediction horizon of 0.5s. To extend the prediction horizon from 0.5s to 1.5s, a three-stage approach has been adopted, in which the model is applied recursively: the second stage operates on the output of the first stage, and the third stage on the output of the second stage. The proposed method has been validated under real-world driving conditions on open roads. In the first experimental scenario, both vehicles interrupt the braking manoeuvre before coming to a complete stop, whereas in the second scenario, both drivers brake until standstill.

As expected, the uncertainty of the prediction increases with the length of the prediction horizon. For this reason, the horizon was limited to 1.5s to keep the distance prediction error within ±0.5m. The aim is to improve situational awareness, enabling an ADAS to intervene as early as possible to reduce the risk of collision or, at least, mitigate its potential consequences. If the vehicle accelerates again before coming to a complete stop, a collision risk assessment system may temporarily flag a risk that does not materialise. However, in safety-critical applications, it is generally better to overestimate the risk than to underestimate it.

Future work will focus on fusing the proposed braking model with additional sources of information in order to estimate the probability of re-acceleration more accurately.

References

[1] Y. F. Payalan and M. A. Guvensan, "Towards next-generation vehicles featuring vehicle intelligence," *IEEE Transactions on Intelligent Transportation Systems*, vol. 21, no. 1, pp. 30–47, 2020.
[2] T. A. Ranney, "Models of driving behavior: A review of their evolution," *Accident Analysis & Prevention*, vol. 26, no. 6, pp. 733–750, 1994.
[3] R. Fuller, "Towards a general theory of driver behaviour," *Accident Analysis & Prevention*, vol. 37, no. 3, pp. 461–472, 2005.
[4] J. N. Russo, T. Sproesser, F. Drouhin, and M. Basset, "Risk level assessment for rear-end collision with Bayesian network," *IFAC-PapersOnLine*, vol. 50, no. 1, pp. 12514–12519, 2017.
[5] S. Lefèvre, D. Vasquez, and C. Laugier, "A survey on motion prediction and risk assessment for intelligent vehicles," *Robotics and Autonomous Systems*, vol. 62, no. 7, pp. 710–721, 2014.
[6] C. Katrakazas, M. Quddus, W.-H. Chen, and L. Deka, "Real-time motion planning methods for autonomous on-road driving," *Transportation Research Part C*, vol. 60, pp. 416–442, 2015.
[7] Y. Bar-Shalom, X. R. Li, and T. Kirubarajan, *Estimation with Applications to Tracking and Navigation*. New York, NY, USA: Wiley, 2001.
[8] S. Thrun, W. Burgard, and D. Fox, *Probabilistic Robotics*. Cambridge, MA, USA: MIT Press, 2005.
[9] B. Paden, M. Čáp, S. Z. Yong, D. Yershov, and E. Frazzoli, "A survey of motion planning and control techniques for self-driving urban vehicles," *IEEE Control Systems Magazine*, vol. 36, no. 2, pp. 20–56, 2016.
[10] N. Deo and M. M. Trivedi, "Convolutional social pooling for vehicle trajectory prediction," in *Proc. IEEE Conf. Computer Vision and Pattern Recognition Workshops (CVPRW)*, 2018, pp. 1468–1476.
[11] F. Altché and A. de La Fortelle, "An LSTM network for highway trajectory prediction," in *Proc. IEEE Intelligent Transportation Systems Conf. (ITSC)*, 2017, pp. 353–359.
[12] B. Kim, S. Kang, and S. Lee, "Probabilistic vehicle trajectory prediction over occupancy grid map via recurrent neural networks," in *Proc. IEEE Intelligent Vehicles Symp. (IV)*, 2017, pp. 399–404.